

# Unconventional Strong Spin-Fluctuation Effects around the Critical Pressure of the Itinerant Ising-Type Ferromagnet URhAl

Yusei Shimizu,<sup>1,\*</sup> Daniel Braithwaite,<sup>1</sup> Bernard Salce,<sup>1</sup> Tristan Combier,<sup>1</sup> Dai Aoki,<sup>1</sup> Eduardo N. Hering,<sup>1</sup> Scheilla M. Ramos,<sup>1</sup> and Jacques Flouquet<sup>1</sup>

<sup>1</sup>*Univ. Grenoble Alpes, INAC-SPSMS, CEA-Grenoble, F-38000 Grenoble, France.*

(Dated: February 3, 2015)

Resistivity measurements were performed for the itinerant Ising-type ferromagnet URhAl at temperatures down to 40 mK under high pressure up to 7.5 GPa, using single crystals. We found that the critical pressure of the Curie temperature exists at around  $P_c \sim 5.2$  GPa. Near  $P_c$ , the  $A$ -coefficient of the  $AT^2$  Fermi-liquid resistivity term below  $T^*$  is largely enhanced with a maximum around 5.2–5.5 GPa. Above  $P_c$ , the exponent of the resistivity  $\rho(T)$  deviates from 2. At  $P_c$ , it is close to  $n = 5/3$ , which is expected by the theory of three-dimensional ferromagnetic spin fluctuations for a 2nd-order quantum-critical point (QCP). However,  $T_C(P)$  disappears as a 1st-order phase transition, and the critical behavior of resistivity in URhAl cannot be explained by the theory of a 2nd-order QCP. The 1st-order nature of the phase transition is weak, and the critical behavior is still dominated by the spin fluctuation at low temperature. With increasing pressure, the non-Fermi-liquid behavior is observed in higher fields. Magnetic field studies point out a ferromagnetic wing structure with a tricritical point (TCP) at  $\sim 4.8$ –4.9 GPa in URhAl. One open possibility is that the switch from the ferromagnetic to the paramagnetic states does not occur simply but an intermediate state arises below the TCP as suggested theoretically recently. Quite generally, if a drastic Fermi-surface change occurs through  $P_c$ , the nature of the interaction itself may change and lead to the observed unconventional behavior.

PACS numbers: 71.27.+a, 75.30.Kz, 75.30.Mb, 75.40.-s

## I. INTRODUCTION

Since the 1960–1970s, the understanding of dynamic critical phenomena and physical properties of itinerant spin-fluctuation systems has been one of the main topics in the fields of magnetism in condensed matter physics<sup>1–6</sup>. This is because these questions lead to understand not only weak itinerant magnetism in  $d$ - and  $f$ -electron systems but also recently observed anomalous non-Fermi-liquid (NFL) behaviors and magnetically mediated Cooper instabilities<sup>7,8</sup> caused by spin fluctuations near quantum-phase transitions (QPTs).

So far, it was widely believed that both itinerant ferromagnetic (FM) and antiferromagnetic (AF) compounds usually have the quantum-critical points (QCPs), where a 2nd-order phase transition occurs at  $T = 0$  by tuning some physical parameter, such as pressure, or atomic substitution, etc. The self-consistent-renormalized (SCR) theory by Moriya and his coworkers gives a theoretical base to describe NFL behaviors of itinerant FM and AF metallic systems near QCPs<sup>6–8</sup>. Furthermore, critical phenomena around magnetic QCPs were investigated theoretically using the renormalization-group method by Hertz<sup>9</sup>, and Millis<sup>10</sup>. Actually, some itinerant AF compounds obey the Moriya–Hertz–Millis theory for critical behaviors near QCPs<sup>11</sup>.

However, for FM quantum criticality, the situation is different. Surprisingly, it has been reported that an almost FM helimagnet, MnSi<sup>12,13</sup>, and several ferromagnets, such as UGe<sub>2</sub><sup>14,15</sup>, and ZrZn<sub>2</sub><sup>17,18</sup>, do not show the QCP at zero field but show a 1st-order phase transition when  $T_C$  is suppressed by applying pressure. To explain these behaviors, recently specific attentions were given to new quantum treatment for FM QPT; for example, Belitz and Kirkpatrick considered particle-hole excitations from a Fermi surface with a low frequency and a long wavelength (soft mode), which cou-

ples to the order parameter<sup>19,20</sup>. They showed that a 2nd-order phase transition at high temperature changes to a 1st-order transition below a *tri-critical point* (TCP) with 1st-order *wing* planes, which terminate at zero temperature in a finite magnetic field, i.e. at a quantum-critical-end point (QCEP)<sup>19,20</sup>. Previously, it has also been discussed that the TCP emerges due solely to the thermal spin fluctuations<sup>21,22</sup> and the magneto elastic coupling<sup>23,24</sup>.

So far, the quantum criticality around the QCEP with the metamagnetic transition has been classified into the same criticality as the QCP for an Ising-type transition<sup>25</sup>. However, there is no symmetry change around a QCEP, whereas the symmetry of the ordered phase is clearly distinguished from the paramagnetic (PM) phase for a QCP. It has recently been pointed out theoretically that the quantum criticality of the metamagnetic transition accompanied with the Fermi-surface change (Lifshitz transition) has another universality class, which differs from other symmetry-breaking phase transitions<sup>26,27</sup>. Also, as unconventional superconductivity associated with FM order has been discovered only in uranium materials (UGe<sub>2</sub><sup>28</sup>, URhGe<sup>29</sup>, and UCoGe<sup>30</sup>), it is intriguing to study the quantum criticality and the spin-fluctuation effects around the FM QPT for itinerant uranium compounds.

Recently, a FM wing structure and a QCEP have been reported for UCoAl, which shows a 1st-order metamagnetic transition at  $\sim 0.7$  T with a FM moment of  $\sim 0.3 \mu_B/U$  at low temperature<sup>31–33</sup>. This compound has a hexagonal ZrNiAl-type structure with space group  $P\bar{6}2m$ , in which there is no inversion symmetry. The uranium atoms form a quasi-Kagomé lattice, thus magnetic frustration effects are possibly expected. From high-pressure studies, it is considered that in UCoAl a TCP exists at negative pressure of  $-0.2$  GPa<sup>34</sup>, and the metamagnetic transition can be explained by the FM wings<sup>32</sup>.

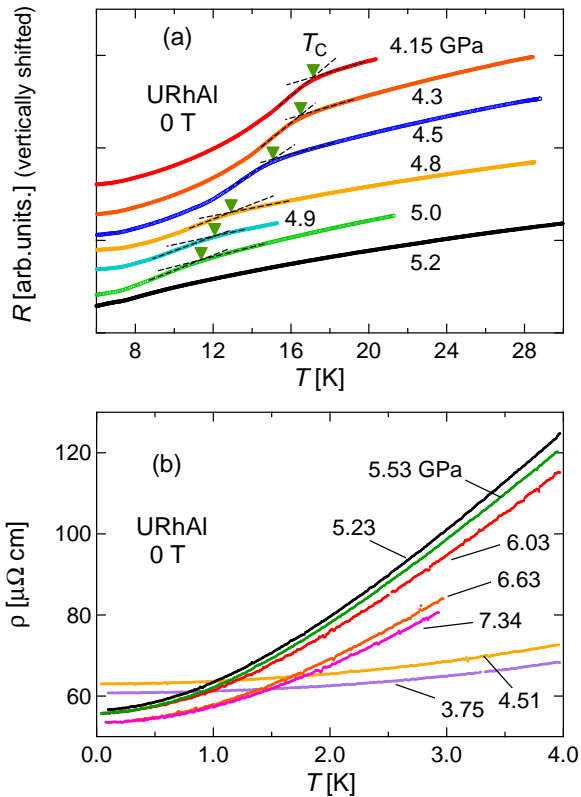


FIG. 1: (Color online) (a) Temperature dependence of resistance (vertically shifted) of URhAl (sample #1) between 6 and 30 K, measured at zero field and high pressures, 4.15, 4.3, 4.5, 4.8, 4.9, 5.0, and 5.2 GPa. The arrows indicate the Curie temperatures ( $T_C$ ) at each pressure. The dashed lines are guides to the eyes. (b) Temperature dependence of resistivity of URhAl (sample #1) below 4 K, measured at zero field and high pressures, 3.75, 4.51, 5.23, 5.53, 6.03, 6.63, and 7.34 GPa.

Since the TCP in UCoAl is estimated to exist at a negative pressure, it is not observable from hydrostatic-pressure measurements. In order to understand the critical phenomena near the itinerant FM QPTs, further experimental examples are necessary.

In this paper, we report pressure-induced quantum criticality of a 5f itinerant Ising-type FM compound, URhAl, which has the same crystal structure as that of UCoAl. URhAl shows a FM transition at 25-27 K at ambient pressure<sup>36-38</sup>, and the FM moment ( $\sim 0.9 \mu_B/U$ ) is strongly Ising-type with the magnetization-easy axis along  $c$ , similar to the Ising-type metamagnetism in UCoAl. The atomic radius of Rh is larger than that of Co, so the 5f-electronic state in URhAl may correspond to a state in which negative pressure is applied for UCoAl<sup>35</sup>. Therefore, the high-pressure study of critical behaviors for URhAl can help to understand the metamagnetism in UCoAl as well as the general problem of FM quantum criticality.

## II. EXPERIMENTAL PROCEDURES

Single crystals of URhAl were grown by the Czochralski pulling method in a tetra-arc furnace. Resistivity measurements under high pressure were performed by using diamond-anvil cells with an *in situ* pressure-tuning device<sup>39,40</sup>. We measured resistivity of samples (#1 and #2) which were less than the size of  $\sim 200 \times 100 \times 30 \mu\text{m}^3$ . The sample geometry did not allow a precise determination of the form factor of resistivity. Therefore, we extrapolated  $A(P)$  linearly to 0 GPa, and obtained absolute values of  $\rho(T, H)$  and  $A$  by normalizing the extrapolated value [ $A(P = 0)$ ] to the zero-pressure value ( $A = 0.27 \mu\Omega\text{ cm/K}^2$  for  $J \perp c$ ), since the pressure variation of  $A$ -coefficient is almost linear for  $P < 4.8$  GPa.

The low- $T$  measurements were carried out for sample #1 using a  $^3\text{He}-^4\text{He}$  dilution refrigerator in temperatures down to 40 mK and in fields up to 7 T under high pressures up to 7.5 GPa. Here, the magnetic field was applied almost along the  $c$ -axis (easy-magnetization axis) and the current was applied perpendicular to the field direction. The high- $T$  measurements under high pressure were performed at zero magnetic field using  $^4\text{He}$  cryostat for sample #1 as well as #2 to check the reproducibility.

As a pressure transmitting medium, liquid argon was used, and pressure was determined with the ruby fluorescence technique. For high- $T$  measurements, since there is a volume increase of helium gas in bellows of the pressure-tuning device above liquid-helium temperature, this may cause a slight change of the force, which is applied to the pressure cell. Then, the determination of pressure is more precise for low- $T$  measurements below  $\sim 4$  K than for high- $T$  measurements above  $\sim 5$  K.

## III. RESULTS AND DISCUSSION

In order to examine the pressure dependence of the Curie temperature of URhAl, we first show the temperature dependence of the resistance at various pressures (shifted vertically) between 6 and 30 K in Fig. 1(a). One can see the clear kink anomaly in the resistivity curves due to the FM transition at the Curie temperature ( $T_C$ ), as indicated by the arrows [Fig. 1(a)].  $T_C$  shifts to lower temperature with increasing pressure, and the kink anomaly becomes too broad to determine  $T_C$  for  $P > 5.0$  GPa.

Figure 1(b) shows results of resistivity measurements below 4 K at high pressures from 3.75 to 7.34 GPa. At 3.75 and 4.51 GPa,  $T_C$  is 19 and 17 K, respectively, and URhAl is FM in the temperature range of Fig. 1(b) at these pressures. The variation of resistivity  $\rho(T)$  is small at low temperature in the FM state. On the other hand, from 5.2 to 7.3 GPa, the variation of resistivity is very large compared to that at 3.75 and 4.51 GPa. Since we did not observe the kink anomaly in the resistivity due to the FM transition above 5.2 GPa, URhAl appears to be PM in the high-pressure region above 5.2 GPa.

Figure 2 shows the obtained  $T$ - $P$  phase diagram at zero field. There is no significant sample dependence of  $T_C(P)$ .

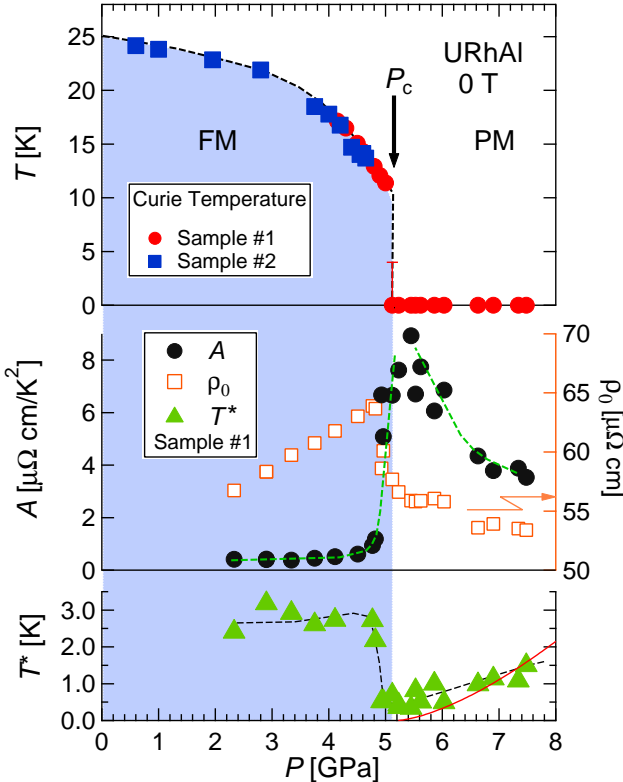


FIG. 2: (Color online)  $T$ - $P$  phase diagram of URhAl at zero field for the samples #1 and #2. The dashed lines are guides to the eyes. The  $A$ -coefficient and the residual resistivity of the sample #1 are also plotted. The solid curve indicates  $T^*(P) \propto (P - P_c)^{3/2}$ , which is predicted by the spin-fluctuation theory for a 2nd-order FM QCP<sup>10,41</sup>.

$T_C(P)$  suddenly disappears above 5.0 GPa. Our results suggest that the FM critical pressure exists at  $P_c \sim 5.2$  GPa.

In Fig. 2, we also plot the  $A$ -coefficient and the residual resistivity  $\rho_0$  as a function of pressure, where  $\rho(T) = \rho_0 + AT^2$ . The pressure variation of the  $A$ -coefficient is very small ( $A \sim 0.4\text{-}0.5 \mu\Omega\text{cm}/\text{K}^2$ ) for  $P < 4.8$  GPa, whereas it shows a drastic increase above 5.0 GPa. The  $A$ -coefficient becomes a maximum ( $A \sim 9 \mu\Omega\text{cm}/\text{K}^2$ ) at around 5.2–5.5 GPa, suggesting a large enhancement of the density of states at Fermi energy [ $D(\epsilon_F)$ ] of itinerant electrons above  $P_c$ . Interestingly, the large increase of the  $A$ -coefficient ( $A \sim 4 \mu\Omega\text{cm}/\text{K}^2$ ) beyond  $P_c$  indicates that the large enhancement of  $D(\epsilon_F)$  remains up to  $\sim 7.5$  GPa (Fig. 2). The behavior of the residual resistivity,  $\rho_0(P)$ , accompanies the behavior of the  $A$ -coefficient,  $A(P)$ . Below 4.8 GPa,  $\rho_0(P)$  increases with increasing pressure almost linearly, then suddenly decreases with increasing pressure above 4.9 GPa. At 0 T  $\rho_0(P)$  shows a step-like behavior at  $\sim 4.8$  GPa slightly below  $P_c \sim 5.2$  GPa.

We also plot  $T^*$ , the maximum temperature for the  $T^2$ -regime, in the 3rd panel of Fig. 2.  $T^*$  is about  $\sim 2\text{-}3$  K in the low-pressure region below  $P_c$ , but it suddenly decreases at  $P_c$ , where  $T^*(P)$  shows a minimum ( $T^* \sim 0.4$  K), and then gradually increases with increasing pressure.

In FM spin fluctuation frame with a 2nd-order QCP,  $T^*(P)$

TABLE I: The  $A$ -coefficient of resistivity,  $A$  [ $\mu\Omega\text{cm}/\text{K}^2$ ], the electronic specific-heat coefficient  $\gamma$  [ $\text{mJ}/\text{K}^2\text{mol}$ ], and the values of  $A/\gamma^2$  [ $\mu\Omega\text{cm}(\text{molK})^2/(\text{mJ})^2$ ] for URhAl, UCoAl<sup>32</sup>, and UGe<sub>2</sub><sup>44</sup>. Here,  $A(0)$  is the value of  $A$ -coefficient at ambient pressure at zero field.

	$P$ [GPa]	$A$	$\gamma$	$A/\gamma^2$	$A/A(0)$
URhAl	0 (FM)	0.27	75	$4.8 \times 10^{-5}$	–
	$P_c \sim 5.2$	8			30
UCoAl	0	0.28	75	$5.0 \times 10^{-5}$	–
	0.54	0.2			0.7
	$P_{\text{QCEP}} \sim 1.5, 7$ T	0.4			1.4
UGe <sub>2</sub>	0	0.007	30	$7.8 \times 10^{-6}$	–
	1.3	0.1	110	$8.3 \times 10^{-6}$	14.3

and  $A(P)$  are predicted to vary as  $T^*(P) \propto (P - P_c)^{3/2}$  and  $A(P) \propto (P - P_c)^{-1}$ , respectively, leading to  $A \propto (1/T^*)^{2/3}$ ; in other words,  $A \times (T^*)^{2/3}$  is constant<sup>10,41</sup>. For URhAl, we obtain  $A \sim 8 \mu\Omega\text{cm}/\text{K}^2$  and  $T^* \sim 0.4$  K at  $P_c$ , leading to  $A \times (T^*)^{2/3} \sim 4.3$ , and  $A \sim 3.5 \mu\Omega\text{cm}/\text{K}^2$  and  $T^* \sim 1.5$  K at 7.5 GPa, leading to  $A \times (T^*)^{2/3} \sim 4.6$ . This rough estimation suggests that the observed large  $A$ -coefficient emerges due to the FM spin-fluctuation effects. However, we would like to point out the peculiarity of critical behavior of the FM QPT in URhAl; as shown in the 3rd panel of Fig. 2,  $T^*(P)$  does not vary as  $T^*(P) \propto (P - P_c)^{3/2}$  (the solid curve) and does not go to zero as  $P \rightarrow P_c$ . Also, the fact that  $T^*$  is finite at  $P_c$  conflicts with presence of a 2nd-order QCP in URhAl.

The maximum value of  $A \sim 9 \mu\Omega\text{cm}/\text{K}^2$  in URhAl near  $P_c$  is quite large for uranium intermetallic compounds. While the heavy-electron superconductor UBe<sub>13</sub> shows the exceptionally large  $A$ -coefficient ( $\sim 90\text{-}100 \mu\Omega\text{cm}/\text{K}^2$ )<sup>42,43</sup>, a lot of uranium compounds show the  $A$ -coefficient of less than  $\sim 1 \mu\Omega\text{cm}/\text{K}^2$  as summarized in the Kadowaki-Woods plot<sup>43</sup>. Table I shows the  $A$ -coefficient, the electronic specific-heat coefficient ( $\gamma$ ), and the ratio  $A/\gamma^2$  for URhAl<sup>38</sup>, UCoAl<sup>32</sup>, and UGe<sub>2</sub><sup>44</sup>. Besides,  $A/A(0)$  indicates the ratio of  $A$  divided by the  $A$ -coefficient at 0 GPa and zero field, i.e.  $A(0)$ . As for UCoAl, the  $A$ -coefficient is  $A \sim 0.28 \mu\Omega\text{cm}/\text{K}^2$ , and the electronic specific-heat coefficient is  $\gamma \sim 75 \text{ mJ}/\text{K}^2\text{mol}$ <sup>32</sup>. The  $A$ -coefficient of UCoAl increases near the QCEP ( $\sim 1.5$  GPa, 7 T)<sup>32</sup>, but the enhancement of  $A$  is not so large compared to the pressure-induced large  $A$ -coefficient in URhAl. Also, the  $A$ -coefficient of UGe<sub>2</sub> increases  $\sim 14$ -fold under high pressure, but the maximum value of  $A$ -coefficient is not so large ( $\sim 0.1 \mu\Omega\text{cm}/\text{K}^2$ ) at  $\sim 1.3$  GPa<sup>44</sup>. On the other hand, a large  $A$ -coefficient ( $\sim 5 \mu\Omega\text{cm}/\text{K}^2$ ) near the critical pressure has been reported in an itinerant heavy-electron FM compound U<sub>4</sub>Ru<sub>7</sub>Ge<sub>6</sub><sup>45</sup>. The observed large  $A$ -coefficient in URhAl near  $P_c$  is comparable with the value observed in cerium heavy-electron compounds such as CeCu<sub>2</sub>Si<sub>2</sub><sup>43,46</sup>. From the comparison with other heavy-electron materials using the Kadowaki-Woods relation, the quantum critical region in URhAl may be described grossly by the strongly correlated heavy quasiparticle with the large  $D(\epsilon_F)$  caused by

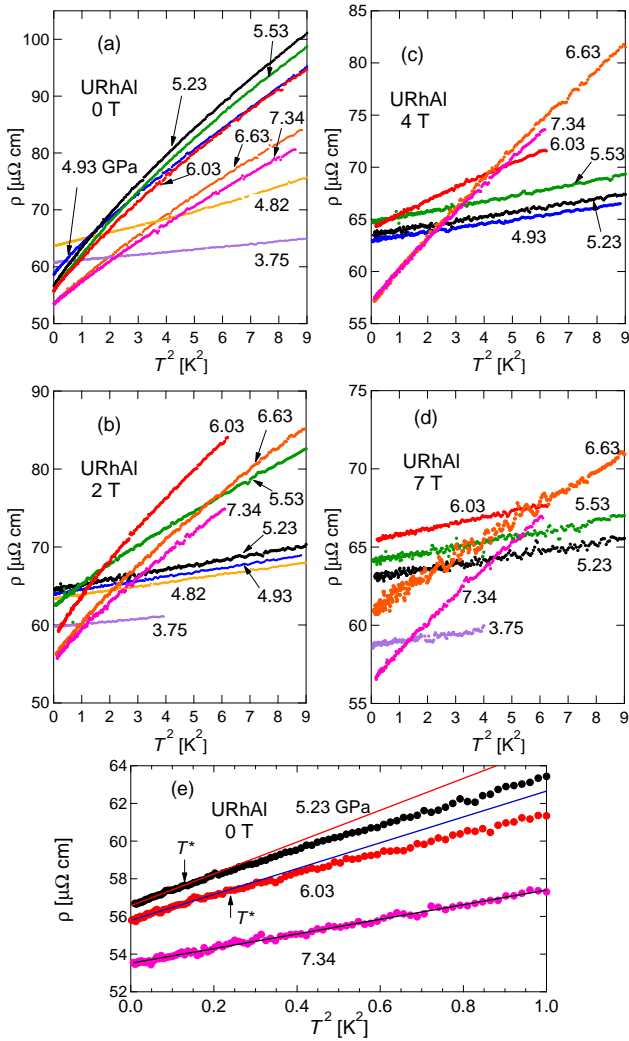


FIG. 3: (Color online)  $\rho(T)$  vs  $T^2$  plot of URhAl (sample #1) at high pressures from 3.75 to 7.34 GPa in (a) 0 T, (b) 2 T, (c) 4 T, and (d) 7 T. (e) The enlarged figure of  $\rho(T)$  curves for 0 T measured at 5.23, 6.03, and 7.34 GPa as a function of  $T^2$  below 1 K. The arrows indicate  $T^*$  (Fig. 2), below which the  $T^2$ -regime works. Here,  $T^*$  at 7.34 GPa is about  $\sim 1.1$  K. The solid lines are the results of fitting by  $\rho(T) = \rho_0 + AT^2$ .

spin fluctuations. However, we should be careful about the above discussion since the value of  $A/\gamma^2$  is not universal depending on the correlation of the system<sup>47-49</sup>.

Next, we shall see low- $T$   $\rho(T)$  curves in zero field and magnetic fields. Figures 3(a), (b), (c), and (d) show the resistivity  $\rho(T)$  vs  $T^2$  under high pressures from 3.75 to 7.34 GPa for 0, 2, 4, and 7 T, respectively. For zero field, at lower pressures than 4.8 GPa, we find  $\rho(T) = \rho_0 + AT^2$  behavior, as predicted for an itinerant FM state at low temperature ( $T \ll T_C$ )<sup>50</sup>. On the other hand, the resistivity shows a remarkable variation with a large increase of the slope ( $A$ -coefficient) at 0 T between 4.82 and 4.93 GPa. Around 5-6 GPa, the temperature region where the resistivity can obey the expression  $\rho(T) = \rho_0 + AT^2$  is much smaller than at 4.82, and 3.75 GPa. In Fig. 3(e), we show the enlarged figure of  $\rho(T)$  curves

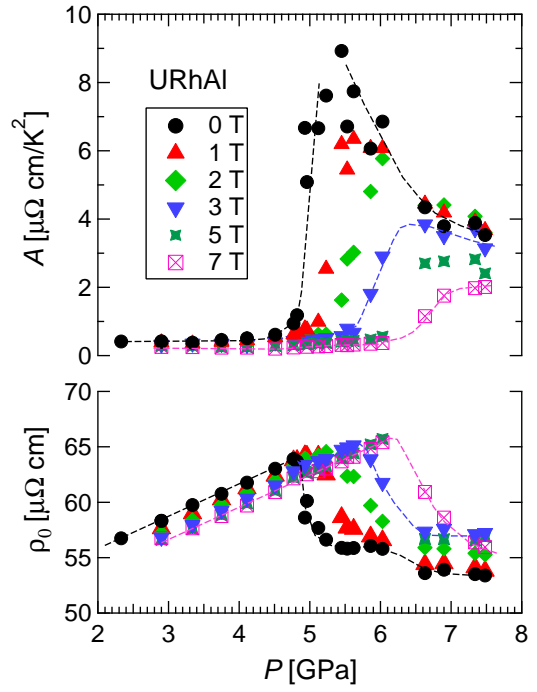


FIG. 4: (Color online) Pressure dependence of the  $A$ -coefficient and the residual resistivity  $\rho_0$  of URhAl (sample #1) in zero and magnetic fields, obtained from the expression,  $\rho(T) = \rho_0 + AT^2$ . The dashed lines are guides to the eyes.

for 0 T measured at 5.23, 6.03, and 7.34 GPa as a function of  $T^2$ . The arrows indicate the temperature,  $T^*$  (Fig. 2), below which the  $T^2$ -regime works. For an applied field of 2 T, the large  $A$ -coefficient is suppressed at 4.93, and 5.23 GPa, and  $\rho(T)$  shows the  $T^2$ -temperature dependence, similar to that at 4.82, and 3.75 GPa. On the other hand, the slope of  $\rho(T)$  becomes large at around 6-6.6 GPa at 2 T. For 4 T, and 7 T, the variation of  $\rho(T)$  at high-pressure region above  $\sim 6.6$  GPa becomes larger than for pressures below  $\sim 6.0$  GPa.

In Fig. 4, we summarize the pressure dependence of the  $A$ -coefficient and the residual resistivity  $\rho_0$  of URhAl (sample #1), obtained from the expression,  $\rho(T) = \rho_0 + AT^2$ , in zero and magnetic fields. With increasing magnetic field, the divergence of the  $A$ -coefficient is suppressed, and the step-like behavior of  $\rho_0$  becomes broad (Fig. 4).

Since the behaviors of the  $A$ -coefficient and  $\rho_0$  above 5.0 GPa differ evidently from those below  $\sim 5.0$  GPa in the FM state, it is considered that URhAl is *not* in the FM state any more above 5.0 GPa. This is consistent with the fact that the anomaly due to the FM transition disappears above 5.0 GPa (Fig. 2). The Curie temperature,  $T_C(P)$ , possibly becomes a 1st-order phase transition, and then  $T_C(P)$  suddenly collapses above 5.0 GPa.

The experimentally observed large enhancement of the  $A$ -coefficient suggests a large mass enhancement due to spin-fluctuation effects and/or a variation of Fermi surface. Generally, large fluctuation effects occur for a 2nd-order phase transition with a divergence of the correlation length of the

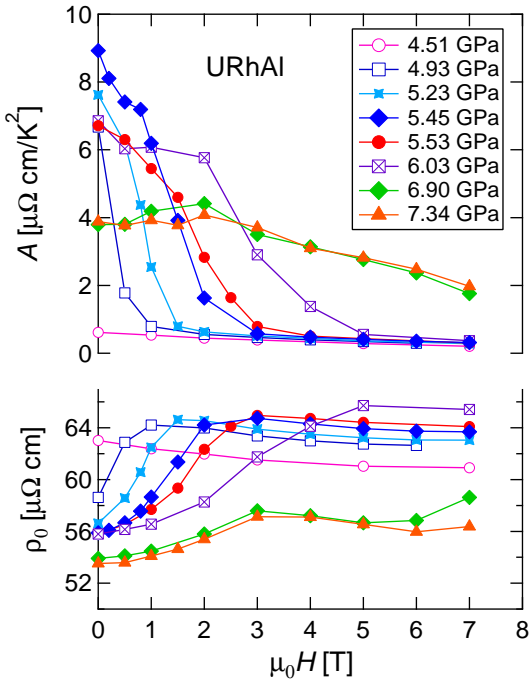


FIG. 5: (Color online) Magnetic-field dependence of the  $A$ -coefficient and the residual resistivity  $\rho_0$  of URhAl (sample #1), obtained from the expression,  $\rho(T) = \rho_0 + AT^2$ .

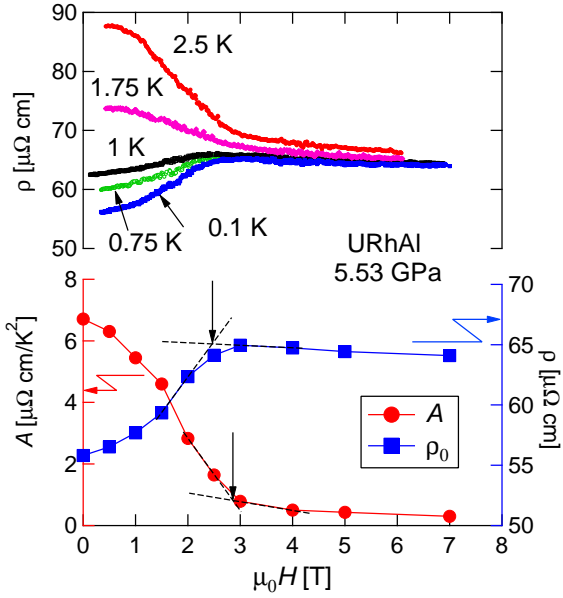


FIG. 6: (Color online) Magnetic field dependence of resistivity of URhAl for the sample #1, measured at 5.53 GPa. The dashed lines are guides to the eyes.

magnetic order. In contrast, such an effect would not be expected for a 1st-order phase transition. Nevertheless, if the transition near the  $P_c$  is only weakly 1st-order and the drop of the FM moment at the FM-PM phase transition is very small, the critical behavior becomes similar to that of a QCP, and

then a large maximum in the  $A$ -coefficient may emerge due to the increase of correlation length as  $T \rightarrow 0$ .

Figure 5 shows the  $A$ -coefficient and the residual resistivity as a function of magnetic field. At 4.5 GPa,  $A(H)$  value is very small, and  $A(H)$  monotonically decreases with increasing field. At 5.0 GPa, the  $A$ -coefficient begins to increase in zero and low fields, and  $A(H)$  is suddenly suppressed by magnetic field of  $\sim 1$  T. At around 5.2–5.5 GPa, the  $A$ -coefficient is very large in zero field and remains large up to 1–1.5 T, then rapidly decreases at high fields (1.5–2 T). At 6.0 GPa, the decrease of  $A(H)$  occurs at higher field near 3 T. At 6.9 and 7.3 GPa, the value of  $A$ -coefficient at 0 T becomes about half of the  $A$  value at 5.5 GPa, and after showing a slight maximum at around 2 T, it monotonically decreases with increasing field. At 6.9 and 7.3 GPa,  $\rho_0(H)$  increases with increasing field, and shows a smooth maximum at around 3 T.

To search for the FM wing structure, we look at the magnetic field dependence of the resistivity [ $\rho(H)$ ] under high pressure. Figure 6 shows  $\rho(H)$  under 5.53 GPa at 2.5, 1.75, 1, 0.75, and 0.1 K with  $A(H)$  and  $\rho_0(H)$  obtained from the temperature dependence of  $\rho(T) = \rho_0 + AT^2$ .  $\rho(H)$  curve bends at around 2.5–3 T for each temperature. We define the anomaly at  $H_m$  at  $T \rightarrow 0$  from  $A(H)$  and  $\rho_0(H)$  as indicated by the arrows in Fig. 6. At the low-field region below  $H_m$ , the  $A$ -coefficient is very large compared to the high-field region above  $H_m$ . On the other hand, the high-field region above  $H_m$  corresponds to the FM side, where the resistivity obeys  $\rho(T) = \rho_0 + AT^2$  with the small  $A$ -coefficient.

The anomaly in  $\rho(H)$  curves supports the presence of FM wing structure in URhAl. In Fig. 7(a), we plot the  $P$ - $H$  phase diagram for  $H_m$  obtained from the magnetic field dependences of  $A$ -coefficient and  $\rho_0$ . We obtain the relation  $\mu_0 dH_m/dP \sim 3.5 \pm 0.1$  T/GPa. Then we estimate the TCP at  $P_{TCP} \sim 4.8$ –4.9 GPa, when  $H_m \rightarrow 0$ , using the value of  $\mu_0 dH_m/dP$ . In UCoAl, which has the same crystal structure as URhAl, a clear 1st-order metamagnetic transition is seen at  $H_m$  due to the FM wing. According to high pressure studies<sup>32</sup>, the metamagnetic transition field of UCoAl varies as  $\mu_0 dH_m/dP \sim 3.5$  T/GPa<sup>32</sup>, which is very similar to that of URhAl. We summarize the values of  $P_{TCP}$  and  $\mu_0 dH_m/dP$  in Table. II.

TABLE II: The values of  $P_{TCP}$  and the slope of the FM wing, i.e.  $\mu_0 dH_m/dP$  for URhAl and UCoAl<sup>32</sup>.

	$P_{TCP}$ [GPa]	$\mu_0 dH_m/dP$ [T/GPa]
URhAl	4.8–4.9	$3.5 \pm 0.1$
UCoAl	–0.2	3.5

When we cross the FM wing, we expect the 1st-order PM–FM phase transition at  $H_m$ . At the 1st-order transition in UCoAl, the  $A$ -coefficient shows a step-like behavior as a function of magnetic field<sup>32</sup>. On the other hand, the step-like behavior in the  $A$ -coefficient of URhAl near  $H_m$  is rather broad. This may indicate that the transition at  $H_m$  is weakly 1st-order in URhAl. However, the sample quality can be the origin of the broadness of the transition.

We shall compare  $A(H)$  for URhAl with that for UCoAl.

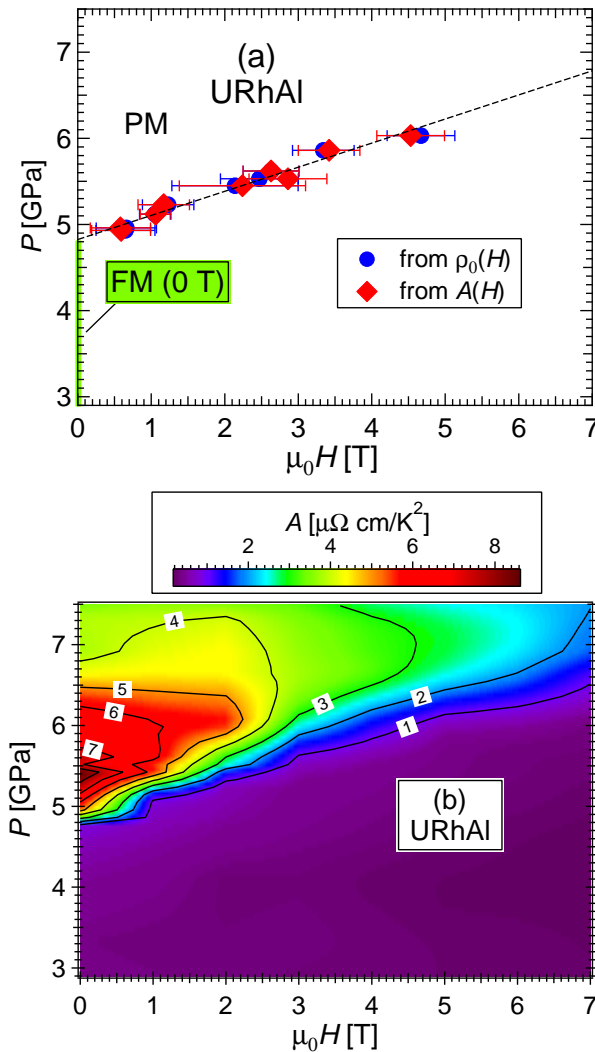


FIG. 7: (Color online) (a) Plot of the observed anomalies in  $A(H)$  and  $\rho(H)$  of URhAl on the  $P$ - $H$  phase diagram for the sample #1. The dashed line indicates the result of liner fitting. (b) Contour plot of the  $A$ -coefficient of resistivity on URhAl on the  $P$ - $H$  phase diagram, obtained from the expression  $\rho(T) = \rho_0 + AT^2$  for the sample #1.

For UCoAl, a step-like behavior in  $A(H)$  at  $H_m$  is seen under low pressure region below 0.54 GPa. For 0.54 GPa, the difference of pressure from the TCP ( $\sim -0.2$  GPa) is estimated to be  $\delta P \equiv P - P_{TCP} \sim 0.74$  GPa. Since we estimate  $P_{TCP} \sim 4.8$  GPa for URhAl in the present work, the pressure of 0.54 GPa in UCoAl may correspond to a pressure of  $4.8 + \delta P \sim 5.54$  GPa in URhAl. At  $\sim 5.5$  GPa, we obtain  $H_m \sim 2.5$  T for URhAl from Fig. 7(a), which is close to the value of  $H_m$  for UCoAl at 0.54 GPa.

In contrast, the enhancement of the  $A$ -coefficient in URhAl is much larger than the value in UCoAl (see, Table I), suggesting that the density of states (mass enhancement and/or the change of Fermi surface) near the QPT is more drastic in URhAl than UCoAl. In URhAl, the  $A$ -coefficient below  $H_m$

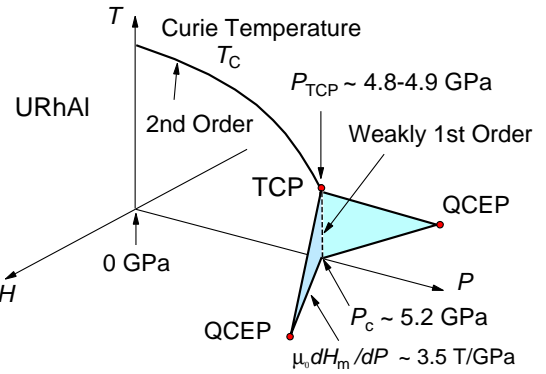


FIG. 8: (Color online) Schematic  $T$ - $P$ - $H$  phase diagram of the FM wings in URhAl [See also the top panel of Fig. 2 and Fig. 7(a)].

at  $\sim 5.0$  GPa is about 20 times larger than the  $A$ -coefficient above  $H_m$  (Fig. 5). In UCoAl, on the other hand, the  $A$ -coefficient in the PM state below  $H_m$  is about only 2 times larger than the  $A$ -coefficient above  $H_m$  at 0 and 0.54 GPa<sup>32</sup>.

The difference of the  $A$ -coefficient between URhAl and UCoAl may be related to that of the magnetic ordered moments; the FM ordered moment in URhAl is 3 times larger ( $\sim 0.9 \mu_B/U$ ) than the magnetic-field-induced FM moment ( $\sim 0.3 \mu_B/U$ ) in UCoAl. As shown theoretically by Yamada<sup>21</sup>, thermally fluctuating magnetic moments enhance the scattering of quasiparticles in the PM state, and may cause such a large  $A$ -coefficient. At present, the ordered moment near  $P_c$  has not yet been studied for URhAl, so further studies are necessary to clarify this point.

The behavior of the  $A$ -coefficient changes in association with the wing structure. To see the relationship between the enhancement of  $A$ -coefficient and the FM wing, it is intriguing to see the contour plot of  $A$ -coefficient on the  $P$ - $H$  phase diagram. Figure 7(b) shows the contour plot of the  $A$ -coefficient on the  $P$ - $H$  phase diagram, obtained from  $\rho(T) = \rho_0 + AT^2$ . The red-colored region in this plot shows the enhancement of the  $A$ -coefficient, whereas the purple-colored region shows the small  $A$ -coefficient. The  $A$ -coefficient is largest at around 5.2-5.5 GPa in zero field. With increasing pressure and magnetic field, the  $A$ -coefficient is suppressed. The large enhancement of  $A$ -coefficient occurs outside of the FM wing (red region).

In Fig. 8, we plot the schematic  $T$ - $P$ - $H$  phase diagram of the FM wings in URhAl [See also the top panel of Fig. 2 and Fig. 7(a)]. The theoretically suggested 1st-order wing planes terminate at the QCEP at zero temperature in a finite field. In UCoAl the magnetic-field dependence of  $A(H)$  coefficient shows a sharp maximum at the PM-FM transition near the QCEP ( $P \sim 1.5$  GPa in  $H \sim 7$  T)<sup>32,38</sup>. Such a field enhancement in  $A(H)$  was not observed in the present work, suggesting that the QCEP of URhAl may exist above  $\sim 7$  T. Alternatively, the interplay between spin fluctuation and Fermi-surface instability can lead to complex phenomena as discussed later.

As close to the critical pressure, the temperature range for

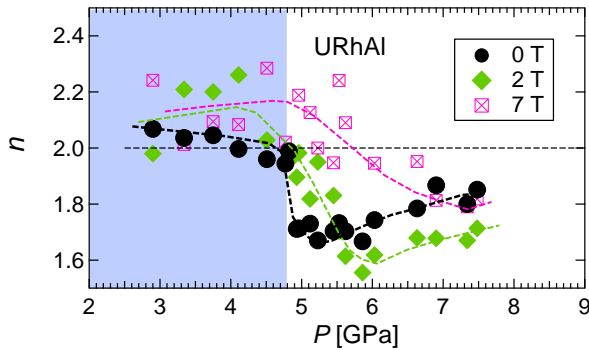


FIG. 9: (Color online) Pressure dependence of the exponent ( $n$ ) of resistivity [ $\rho(T) = \rho_0 + A'T^n$ ] for URhAl (sample #1) at 0, 2, and 7 T. The dashed lines are guides to the eyes.

Fermi-liquid regime [ $\rho(T) = \rho_0 + AT^2$ ] is found to be very small ( $T^* \sim 0.4$  K), an alternative description is to focus on the NFL behavior. We analyzed the resistivity data by the expression,  $\rho(T) = \rho_0' + A'T^n$ . Here, the maximum temperature for the NFL regime  $\rho(T) = \rho_0' + A'T^n$ , i.e.,  $T^{**} \sim 2.2$  K at  $\sim P_c$ . Figure 9 shows the pressure dependence of the exponent of resistivity ( $n$ ). As seen in Fig. 9, at 0 T the exponent  $n$  is about 2 below 4.8 GPa, whereas  $n(P)$  decreases with a step-like variation to a minimum at around  $\sim 5.0$ -6.0 GPa. At around  $\sim 5.0$ -6.0 GPa, the values of  $n$  are about 1.6-1.8. At 2 T and 7 T, the step-like behavior and the minimum of the exponent  $n(P)$  shift to higher pressure regions. At 7 T, the dip of  $n(P)$  at around  $\sim 7.0$  GPa becomes shallow and broad, and the value of  $n(P)$  becomes slightly larger than at 0 T and 2 T.

The exponent  $n$  (Fig. 9) varies as a function of pressure corresponding to the behavior of the  $A$ -coefficient (Fig. 4). Above  $P_c$ , the exponent  $n$  is nearly 1.6-1.7, which is close to the value ( $n = 5/3$ ) suggested from the SCR theory for three-dimensional FM spin fluctuation near a QCP. However, this NFL behavior seems to conflict with the presence of the FM 1st-order wing structure in URhAl. A weakly 1st-order nature at the FM wing may explain the NFL behavior in the resistivity.

Hereafter, we note that the critical behavior around  $P_c$  in URhAl is different from the theoretical suggestion for a 2nd-order FM QCP. It is suggested that the ratio of  $T^*$  for the Fermi-liquid regime to  $T^{**}$  for the NFL regime is enhanced as  $T^{**}/T^* \propto (P - P_c)^{-3/4}$  as approaching  $P_c$  for a 2nd-order FM QCP<sup>10,41</sup>. For URhAl,  $T^{**}$  does not change clearly, i.e.,  $T^{**} \sim 2.1 \pm 0.2$  K. In addition,  $T^*(P)$  is almost linear (Fig. 2). These experimental results for URhAl suggest that the spin-fluctuation effects cannot be explained simply by the 2nd-order FM QCP again.

In URhAl, the NFL properties (see Fig. 9) are observed far above  $P_c$ , and the pressure domain of the enhancement of the  $A$ -coefficient appears quite asymmetric around  $P_c$ . Furthermore the enhancement of the  $A$ -coefficient extends over a large  $P$  window (5.5-7 GPa). Then the key question is if the switch from the FM state to the PM state simply occurs

at  $P_c$  or if there is a mark of a new pressure-induced phase intermediate between the FM and the PM phases.

Recently it has been shown theoretically that another new phase possibly stabilizes near the FM-PM QPT<sup>51-56</sup>; if there are quantum fluctuations in terms of fermionic particle-hole excitations on the Fermi surface, some deformations of the Fermi surface enhance the phase space available for the quantum fluctuations, and such a Fermi-surface instability causes another type of ordering to gain the free energy of the system<sup>53-56</sup>.

It has been shown that two cases of new ordering are possible near the FM-PM QPT: (i) spiral magnetic phase, and (ii) spin-nematic phase<sup>54</sup>. The energy scale of the spin-nematic phase transition is almost 10 times smaller than the case of spiral magnetic phase<sup>54</sup>, therefore a spiral magnetic phase might be more likely to occur. A spiral magnetic phase emerges *below* the TCP as an *intermediate state* between the uniform FM and the PM states<sup>54,55</sup>. The transition between the uniform FM and the spiral magnetic states occurs as a Lifshitz transition, whereas the transition between the spiral magnetic state and the PM state is of 1st-order<sup>54</sup>. Interestingly, an anisotropic dispersion for electron band changes the nature of the spiral-to-PM phase transition, and the transition possibly becomes 2nd-order<sup>54</sup>.

The possible presence of the intermediate new phase might explain why we cannot see a clear 1st-order transition between the FM and the PM states above  $P_c$ , different from the case of UCoAl. In order to explore such a new phase around the QPT, further experimental studies are required. In particular, measurements of thermodynamic quantities and observation of Fermi-surface change through  $P_c$  for URhAl, though experimentally challenging, would deepen the understanding the Fermi-surface instability and the nature of the FM QPT.

In URhAl, no superconductivity was observed under high-pressure up to 7.5 GPa at low temperature down to  $\sim 0.1$  K. At present we cannot rule out the possibility that the sample quality affects the emergence of superconductivity and the superconducting transition temperature is too low to be detected. However, even if a superconductivity does not occur, the FM system would resolve the instability due to the quantum fluctuation at  $T \rightarrow 0$  by the occurrence of another new phase associated with the Fermi-surface instability as mentioned just above.

It is interesting to consider why the intermediate phase possibly appears in URhAl. One may consider that the lack of local inversion center and/or the quasi-Kagome lattice in ZrNiAl-type structure can induce the intermediate phase. However, the ZrNiAl-type hexagonal symmetry structure ( $P\bar{6}2m$ :  $D_{3h}^3$ ) does not lead to Dzyaloshinskii-Moriya interaction<sup>57</sup>, which could induce a helimagnetic order<sup>58</sup>. Such an intermediate phase has not yet been observed in UCoAl, which has the same ZrNiAl-type structure, around the PM-FM phase transition induced by uniaxial stress along the  $c$ -axis<sup>59-61</sup>. The relationship between the crystal structure and the occurrence of the intermediate phase remains open question. The authors in Ref.<sup>54</sup> suggest that the intermediate phase may generally occur even for a simple spherical Fermi surface due to the Fermi-surface instability accompanying the quan-

tum fluctuations (particle-hole excitations on the Fermi surface). As seen in Fig. 9, the NFL behavior of the resistivity is remarkable in URhAl far above  $P_c$ . Such strong quantum-fluctuation effects near the FM-PM QPT may invoke the intermediate phase in this material.

#### IV. CONCLUSION

The quantum criticality of the three-dimensional-Ising-type itinerant FM compound URhAl was studied by low-temperature resistivity measurements under high pressure up to 7.5 GPa. The Curie temperature is suppressed with increasing pressure, and suddenly disappears above 5.0 GPa. Our resistivity results suggest the FM critical pressure of  $\sim 5.2$  GPa. Above 5.2 GPa, the ground state is not FM, and the  $A$ -coefficient is largely enhanced at around 5.2-5.5 GPa in zero and low-field region. The characteristics of the temperature

and the magnetic-field dependences of the resistivity may be consistent with the presence of a FM wing structure with an estimated TCP at 4.8-4.9 GPa. At least with the present quality of the crystal the 1st-order phase transition appears weak. The resistivity shows the NFL behavior above 5.0 GPa up to 7.5 GPa. URhAl may be a material in which the switch from the FM state to the PM state occurs through an intermediate phase around the QPT.

#### ACKNOWLEDGMENT

We would like to thank S. Kambe, G. Knebel, K. Ishida, Y. Tada, K. Hattori, S. Hoshino, and Y. Ikeda for valuable discussions and helpful comments. This work was supported by ERC starting grant New Heavy Fermion, KAKENHI, REIMEI, ICC-IMR, and ANR project PRINCESS.

---

\* Electronic address: yuseishimizu@issp.u-tokyo.ac.jp

- <sup>1</sup> S. Doniach, and S. Engelsberg, Phys. Rev. Lett. **17**, 750 (1966).
- <sup>2</sup> N. F. Berk, and J. R. Schrieffer, Phys. Rev. Lett. **17**, 433 (1966).
- <sup>3</sup> M. T. Bléal-Monod, S.-K. Ma, and D. R. Fredkin, Phys. Rev. Lett. **20**, 929 (1968).
- <sup>4</sup> T. Moriya, Phys. Rev. Lett. **24**, 1433 (1970).
- <sup>5</sup> T. Moriya, and A. Kawabata, J. Phys. Soc. Jpn. **34**, 639 (1973).
- <sup>6</sup> T. Moriya and T. Takimoto J. Phys. Soc. Jpn. **64**, 960 (1995).
- <sup>7</sup> T. Moriya, *Spin Fluctuations in Itinerant Electron Magnetism*, Springer-Verlag Berlin Heidelberg GmbH, (1985).
- <sup>8</sup> T. Moriya, and K. Ueda, Rep. Prog. Phys. **66**, 1299 (2003).
- <sup>9</sup> J. A. Hertz, Phys. Rev. B **14**, 1165 (1976).
- <sup>10</sup> A. J. Millis, Phys. Rev. B **48**, 7183 (1993).
- <sup>11</sup> Another alternative is the local criticality picture with the fluctuations for the Fermi surface; see, Löhneysen, A. Rosch, M. Vojta, and P. Wolfle, Rev. Mod. Phys. **79**, 1015 (2007).
- <sup>12</sup> C. Pfeiferer, G. J. McMullan, S. R. Julian, and G. G. Lonzarich, Phys. Rev. B **55**, 8330 (1997).
- <sup>13</sup> C. Pfeiferer, S. R. Julian, and G. G. Lonzarich, Nature **414**, 427 (2001).
- <sup>14</sup> C. Pfeiferer, and A. D. Huxley, Phys. Rev. Lett. **14**, 147005 (2002).
- <sup>15</sup> V. Taufour, D. Aoki, G. Knebel, and J. Flouquet, Phys. Rev. Lett. **105**, 217201 (2010).
- <sup>16</sup> H. Kotegawa, V. Taufour, D. Aoki, G. Knebel, and J. Flouquet, J. Phys. Soc. Jpn. **80**, 083703 (2011).
- <sup>17</sup> M. Uhlaz, C. Pfeiferer, and S. M. Hayden, Phys. Rev. Lett. **93**, 256404 (2004).
- <sup>18</sup> N. Kabeya, H. Maekawa, K. Deguchi, N. Kimura, H. Aoki, and N. K. Sato, J. Phys. Soc. Jpn. **81**, 073706 (2012).
- <sup>19</sup> D. Belitz, T. R. Kirkpatrick, T. Vojta, Phys. Rev. Lett. **82**, 4707 (1999).
- <sup>20</sup> D. Belitz, T. R. Kirkpatrick, and J. Rollbühler, Phys. Rev. Lett. **94**, 247205 (2005).
- <sup>21</sup> H. Yamada, Phys. Rev. B **47**, 11211 (1993).
- <sup>22</sup> H. Yamada, Physica B **391**, 42 (2007).
- <sup>23</sup> V. P. Mineev, J. Phys. Conf. Ser. **400**, 032053 (2012).
- <sup>24</sup> G. A. Gehring, Europhys. Lett. **82**, 60004 (2008).
- <sup>25</sup> A. J. Millis, A. J. Schofield, G. G. Lonzarich, and S. A. Grigera, Phys. Rev. Lett. **88**, 217204 (2002).

- <sup>26</sup> Y. Yamaji, T. Misawa, and M. Imada, J. Phys. Soc. Jpn. **76**, 063702 (2007).
- <sup>27</sup> M. Imada, T. Misawa, and Y. Yamaji, J. Phys.: Condens. Matter **22**, 164206 (2010).
- <sup>28</sup> S. S. Saxena, P. Agarwal, K. Ahilan, F. M. Grosche, R. K. W. Haselwimmer, M. J. Steiner, E. Pugh, I. R. Walker, S. R. Julian, P. Monthoux, G. G. Lonzarich, A. Huxley, I. Sheikin, D. Braithwaite, and J. Flouquet, Nature **406**, 587 (2000).
- <sup>29</sup> D. Aoki, A. Huxley, E. Ressouche, D. Braithwaite, J. Flouquet, J.-P. Brison, E. Lhotel, and C. Paulsen, Nature **413**, 613 (2001).
- <sup>30</sup> N. T. Huy, A. Gasparini, D. E. De Nijs, Y. Huang, J. C. P. Klaasse, T. Gortenmulder, A. De Visser, A. Hamann, T. Görlach, and H. v Löhneysen, PRL **99**, 067006 (2007).
- <sup>31</sup> A. V. Andreev, R. Z. Levitin, Y. F. Popov, and R. Y. Yumaguzhin, Sov. Phys. Solid State, **27**, 1145 (1985).
- <sup>32</sup> D. Aoki, T. Combier, V. Taufour, T. D. Matsuda, G. Knebel, H. Kotegawa, and J. Flouquet, J. Phys. Soc. Jpn. **80**, 094711 (2011).
- <sup>33</sup> T. D. Matsuda, Y. Aoki, H. Sugawara, H. Sato, A. V. Andreev, and V. Sechovsky, J. Phys. Soc. Jpn. **68**, 3922 (1999).
- <sup>34</sup> N. V. Mushnikov, T. Goto, K. Mamishima, H. Yamada, A. V. Andreev, Y. Shiokawa, A. Iwao, and V. Sechovsky, Phys. Rev. B **59**, 6877 (1999).
- <sup>35</sup> A. V. Andreev, I. K. Kozlovskaya, N. V. Mushnikov, T. Goto, V. Sechovsky, Y. Homma, and Y. Shiokawa, J. Alloys Compd. **284**, 77 (1999).
- <sup>36</sup> P. A. Veenhuizen, F. R. de Boer, A. A. Menovsky, V. Sechovsky, and L. Havela, J. Phys. (Paris) **12**, 485 (1988).
- <sup>37</sup> P. Javorský, L. Havela, F. Wastin, P. Boulet, and J. Rebizant, Phys. Rev. B **69**, 054412 (2004).
- <sup>38</sup> T. Combier, Doctoral Thesis, CEA-Grenoble (2014).
- <sup>39</sup> B. Salce, J. Thomasson, A. Demuer, J. J. Blanchard, J. M. Martinod, L. Devouille, and A. Guillaume, Rev. Sci. Instrum. **71**, 2461 (2000).
- <sup>40</sup> A. Demuer, C. Marcenat, J. Thomasson, R. Calemczuk, B. Salce, P. Lejay, D. Braithwaite, and J. Flouquet, J. Low. Temp. Phys. **120**, 245 (2000).
- <sup>41</sup> J. Flouquet, arXiv: cond-mat/0501602 (2005).
- <sup>42</sup> G. Remenyi, D. Jaccard, J. Flouquet, A. Briggs, Z. Fisk, J. L. Smith, and H. R. Ott, J. Phys. (Paris) **47**, 367 (1986).
- <sup>43</sup> K. Kadowaki, and S. B. Woods, Solid. State. Commun. **58**, 507

(1986).

<sup>44</sup> N. Tateiwa, T. C. Kobayashi, K. Hanazono, K. Amaya, Y. Haga, R. Settai, and Y. Onuki, *J. Phys.: Condens. Matter* **13**, L17 (2001).

<sup>45</sup> H. Hidaka, S. Takahashi, Y. Shimizu, T. Yanagisawa, and H. Amitsuka, *J. Phys. Soc. Jpn. Suppl.* **80**, SA102 (2011).

<sup>46</sup> A. Holmes, D. Jaccard, and K. Miyake, *Phys. Rev. B* **69**, 024508 (2004).

<sup>47</sup> The link between the enhancement of  $A$  and  $\gamma$  would not be obvious if the system changes from a weakly correlated coupling ( $\gamma_{\text{cor}} \sim \gamma_{\text{band}}$ ) to a strongly correlated coupling ( $\gamma_{\text{cor}} \gg \gamma_{\text{band}}$ )<sup>48</sup>, where  $\gamma_{\text{band}}$  and  $\gamma_{\text{cor}}$  are the electronic specific-heat coefficient of the electronic band and the contribution from the mass enhancement due to the strong correlation, respectively. Here, the total electronic specific-heat coefficient is  $\gamma \equiv \gamma_{\text{cor}} + \gamma_{\text{band}}$ <sup>48</sup>. For  $\gamma_{\text{cor}} \gg \gamma_{\text{band}}$ ,  $A/\gamma^2 \sim A/\gamma_{\text{cor}}^2$ , whereas for  $\gamma_{\text{cor}} \sim \gamma_{\text{band}}$ ,  $A/\gamma^2 \sim A/(\gamma_{\text{cor}} + \gamma_{\text{band}})^2 < A/\gamma_{\text{cor}}^2$ . Therefore, the value of  $A/\gamma^2$  is not universal depending on the strength of correlation in the system. Recently, it was revealed for the AF heavy-electron compound CeRh<sub>2</sub>Si<sub>2</sub> that the ratio  $A/\gamma^2$  goes from the weak coupling regime to the strong coupling regime around  $P_c$  with increasing pressure<sup>49</sup>.

<sup>48</sup> K. Miyake, T. Matsuura, and C. M. Varma, *Solid. State. Commun.* **71**, 1149 (1989).

<sup>49</sup> A. P. Morales, Doctoral Thesis, CEA-Grenoble (2014).

<sup>50</sup> K. Ueda, and T. Moriya, *J. Phys. Soc. Jpn.* **39**, 605 (1975).

<sup>51</sup> D. L. Maslov, and A. V. Chubukov, *Phys. Rev. B* **79**, 075112 (2009).

<sup>52</sup> A. V. Chubukov, and D. L. Maslov, *Phys. Rev. Lett.* **103**, 216401 (2009).

<sup>53</sup> G. J. Conduit, A. G. Green, and B. D. Simons, *Phys. Rev. Lett.* **103**, 207201 (2009).

<sup>54</sup> U. Karahasanovic, F. Krüger, and A. G. Green, *Phys. Rev. B* **85**, 165111 (2012).

<sup>55</sup> S. J. Thomson, F. Krüger, and A. G. Green, *Phys. Rev. B* **87**, 224203 (2013).

<sup>56</sup> C. J. Pedder, F. Krüger, and A. G. Green, *Phys. Rev. B* **88**, 165109 (2013).

<sup>57</sup> M. Kataoka, and O. Nakanishi, *J. Phys. Soc. Jpn.* **50**, 3888 (1981).

<sup>58</sup> I. E. Dzyaloshinskii, *Sov. Phys. JETP* **19**, 960 (1964).

<sup>59</sup> Y. Ishii, M. Kosaka, Y. Uwatoko, A. V. Andreev, and V. Sechovsky, *Physica B* **334**, 160 (2003).

<sup>60</sup> K. Karube, S. Kitagawa, T. Hattori, K. Ishida, N. Kimura, and T. Komatsubara, *J. Phys. Soc. Jpn.* **83**, 084706 (2014).

<sup>61</sup> Y. Shimizu, B. Salce, T. Combier, D. Aoki, and J. Flouquet, *J. Phys. Soc. Jpn.* **84**, 023704 (2015).